Benzo(*a*)pyrene Quinones Increase Cell Proliferation, Generate Reactive Oxygen Species, and Transactivate the Epidermal Growth Factor Receptor in Breast Epithelial Cells

Andrew D. Burdick, John W. Davis II, Ke Jian Liu, Laurie G. Hudson, Honglian Shi, Michael L. Monske, and Scott W. Burchiel

The University of New Mexico, College of Pharmacy Toxicology Program, Albuquerque, New Mexico

ABSTRACT

Polycyclic aromatic hydrocarbons, such as benzo(*a*)pyrene (BaP), are known mammary carcinogens in rodents and may be involved in human breast cancer. We have reported previously that BaP can mimic growth factor signaling and increase cell proliferation in primary human mammary epithelial cells and the human mammary epithelial cell line MCF-10A. BaP-quinones (BPQs) are important metabolites of BaP that have been associated with the production of reactive oxygen species. Using a model of epidermal growth factor (EGF) withdrawal in MCF-10A, we hypothesized that production of reactive oxygen species by BPQs could lead to the activation of the EGF receptor (EGFR). Here, we demonstrate through electron paramagnetic resonance spectroscopy and flow cytometry that 1,6-BPQ and 3,6-BPQ produce superoxide anion and hydrogen peroxide in MCF-10A cells. Furthermore, we show that BPQs increase EGFR, Akt, and extracellular signal-regulated kinase activity, leading to increased cell number in the absence of EGF. The BPQ-induced EGFR activity and associated cell proliferation were attenuated by the EGFR inhibitor AG1478, as well as by the antioxidant *N*-acetyl cysteine. Overexpression of catalase, but not Cu/Zn superoxide dismutase, reduced the extent of BPQ-dependent increased cell number and EGFR pathway activation. Moreover, the direct treatment of MCF-10A cells with hydrogen peroxide enhanced EGFR, Akt, and extracellular-regulated kinase phosphorylation that could be similarly inhibited by AG1478, *N*-acetyl cysteine, and catalase. Taken together, these data indicate that BPQs, through the generation of hydrogen peroxide, activate the EGFR in MCF-10A cells, leading to increased cell number under EGF-deficient conditions.

INTRODUCTION

Breast cancer is a complex disease with a significant number of genetic and environmental risk factors associated with an increased occurrence (for a review, see Refs. 1 and 2). It has been hypothesized that exposure to environmental pollutants may increase the risk of developing breast cancer. PAHs,[1] such as BaP, are widespread environmental contaminants formed as byproducts of combustion (3). Several lines of experimental evidence have suggested a role for PAHs in breast carcinogenesis. For instance, PAHs have been found to be potent mammary carcinogens in rodents (4, 5), and studies have indicated that chronic exposure of HMEC cultures to BaP may induce a neoplastic phenotype (6).

It is widely believed that BaP requires biological activation through oxidative metabolism to be carcinogenic. The ultimate carcinogenic metabolite has often been considered to be the cytochrome P450 isozyme- and microsomal epoxide hydrolase-derived metabolite 7,8-dihydroxy-9,10-epoxy-7,8,9,10-tetrahydrobenzo(*a*)pyrene (BPDE), which has been found to form stable adducts with DNA (3, 7). BPDE-DNA adducts have been shown to form preferentially at mutational hot spots in the *p53* tumor suppressor gene (8), to initiate a guanine-to-thymidine transversion mutation that activates proto-oncogenic *ras* (9), and have been detected in human breast tumors (10). Although BPDE has been well studied, the mechanism(s) by which BaP metabolites may act as tumor promoters is less well known. A large proportion of the metabolic profile of BaP includes the BPQs that are produced biologically by cytochrome P450 isozymes and peroxidases, as well as environmentally through UV light (11, 12). BPQs are highly chemically active compounds that have been demonstrated in chemical systems to undergo one electron redox cycling with their semiquinone radicals resulting in the formation of superoxide anion (O_2^-), hydrogen peroxide (H_2O_2), and hydroxyl radical (·OH) by Fenton chemistry (collectively, ROS; 13, 14). We and others have hypothesized that many cellular effects of BaP may reflect its metabolism into BPQs and their subsequent ability to generate intracellular ROS (for recent reviews, see Refs. 15–17). Although the substantial formation of ROS has been associated with cell damage and apoptosis (16, 18), recent evidence suggests that low concentrations of endogenous ROS may be essential participants in normal cell signaling, where they act as second messengers (19, 20). ROS signaling often results in the phosphorylation and activation of growth factor receptor pathways. For example, H_2O_2 was demonstrated to increase the tyrosine phosphorylation of the insulin receptor (21) and the EGFR (22). In addition, the signaling mechanism of the EGFR was shown to involve the generation of H_2O_2 (23), and H_2O_2 treatment has led to Erk activation (24) and the EGFR-dependent activation of Akt (25). This evidence indicated that under certain conditions, ROS signaling led to the enhancement of prosurvival pathways by activating growth factor receptors. Therefore, the production of ROS by environmental agents may be of particular importance in tumor promotion, where aberrant activation of growth factor receptor pathways would be detrimental.

We have reported that BaP was mitogenic in primary HMECs cultured in limiting amounts of EGF (26). Similar results were obtained in the spontaneously immortalized, nontumorigenic, growth factor-dependent HMEC line MCF-10A, where BaP increased cell growth in the absence of insulin (27) as well as EGF.[2] In MCF-10A cells, BaP increased PI3-K activity and tyrosine phosphorylation of the insulin-like growth factor I receptor β subunit, insulin receptor

[1] The abbreviations used are: PAH, polycyclic aromatic hydrocarbon; BaP, benzo-(*a*)pyrene; HMEC, human mammary epithelial cell; BPDE, 7,8-dihydroxy-9,10-epoxy-7,8,9,10-tetrahydrobenzo(*a*)pyrene; BPQ, BaP-quinone; ROS, reactive oxygen species; EGF, epidermal growth factor; EGFR, epidermal growth factor receptor; Erk, extracellular signal-regulated kinase; PI3-K, phosphatidylinositol 3′-kinase; BMPO, 5-*tert*-butoxycarbonyl-5-methyl-1-pyrroline-*N*-oxide; EPR, electron paramagnetic resonance spectroscopy; SOD, superoxide dismutase; SOD1, Cu/Zn superoxide dismutase; rt-PCR, reverse transcriptase-PCR; HO-1, heme oxygenase-1; GSK-3, glycogen synthase kinase-3; H_2DCF, 2′,7′-dichlorofluorescein; DA, diacetate; DCF, dichlorofluorescein; CAT, catalase; NAC, *N*-acetyl cysteine; AhR, aryl hydrocarbon receptor; p-Akt, phosphorylated Akt; p-Erk, phosphorylated Erk1,2.

[2] S. W. Burchiel, A. D., Burdick, and J. W. Davis, II, unpublished observations.

substrate-1, and the growth factor receptor adaptor protein Shc (27). These data provided evidence that BaP could mimic growth factor receptor signaling in HMECs, although the specific mechanism by which these pathways were activated was unclear.

In the current studies, we used a previously characterized model of EGF withdrawal in MCF-10A cells (28) to determine whether BPQs could increase cell number and activate EGFR signaling pathways in the absence of exogenously added EGF. Here, we show that BPQs increased EGFR tyrosine phosphorylation, Akt, and Erk1,2 activation and increased cell number in the absence of EGF. Importantly, ROS production by BPQs was correlated with EGFR signaling and BPQ-induced cell proliferation. These findings suggest a potential mechanism by which BaP metabolites can activate growth factor receptors in mammary epithelial cells and may represent one pathway by which BaP acts as a tumor promoter.

MATERIALS AND METHODS

Chemicals. All chemicals were purchased from Sigma (St. Louis, MO), unless otherwise indicated. 1,6-BPQ and 3,6-BPQ were purchased from Midwest Research Institute (Kansas City, MO) at >99% purity and maintained as stock solutions in anhydrous tissue culture grade DMSO. AG1478 was obtained from Calbiochem (San Diego, CA). BMPO was a gift from Dr. B. Kalyanaraman (Medical College of Wisconsin, Milwaukee, WI) and was stored in a stock solution of PBS at $-20°C$. Except where noted, the final concentration of DMSO in all experiments was 0.1%.

MCF-10A Cell Culture. MCF-10A cells were grown on Vitrogen-coated (Collagen Corp., Palo Alto, CA) 100×20-mm dishes (Corning Glass, Corning, NY) in serum-free and growth factor-defined media at 10% CO_2 and 37°C as described previously (28).

Cell Number Determination. Cells were plated into 96-well plates pre-coated with collagen-I (Becton Dickinson, Bedford, MA) at 1000 cells/well. Forty-eight h after plating, cells were treated as indicated in EGF-deficient media. Fresh media and treatments were exchanged every 48 h, where appropriate. Cell number was determined with the CellTiter 96 AQ$_{ueous}$ One Solution Cell Proliferation Assay (Promega) according to supplied instructions. The assay is based on the bioreduction of the 3-(4,5-dimethylthiazol-2-yl)-5-(3-carboxymethoxy-phenyl)-2-(4-sulfonyl)-2H-tetrazolium reagent to a colored formazan product. The absorbance of the product at 490 nm has been reported to be directly proportional to the number of viable cells in culture (29). Results of the colorimetric assays were verified at least once by counting total nuclei with a Coulter counter, as described previously (26). In transfection assays, cells were plated as described above and transiently transfected 48 h after plating with FuGENE 6 transfection reagent (Roche Applied Science, Indianapolis, IN) and 0.05 μg DNA/well. Cells were allowed to recover for 24 h in complete media and then treated as indicated in EGF-deficient media.

Determination of Akt and Erk1,2 Activity. Subconfluent cells were cultured overnight in media without EGF or insulin to reduce basal Akt and Erk1,2 activities and then treated as indicated in similar media. The extent of Akt and Erk1,2 phosphorylation was determined in MCF-10A cells by Western blotting with phosphorylated Akt (Ser^{473}) or phosphorylated Erk1,2 (Thr^{202}/Tyr^{204}) antibodies (Cell Signaling Technologies) detected by chemiluminescence (NEN Renaissance Chemiluminescent Reagent) as described previously (30). Akt kinase activity was measured with a nonradioactive Akt kinase assay kit according to the supplied instructions (Cell Signaling Technologies). Erk1,2 activity was evaluated with the PathDetect *trans*-reporting system (Stratagene, La Jolla, CA) that uses cotransfection of an Elk-1/GAL4 fusion protein with a GAL4-driven luciferase reporter (see Fig. 2 in "Results" for details). Cells were harvested according to Promega's Luciferase Reporter Assay System, and luciferase activity was determined in 96-well opaque plates (Perkin-Elmer Life Sciences, Boston, MA) using a Wallac Victor2 1420 multilabel plate reader (Perkin-Elmer) and normalized to total cellular protein (Pierce bicinchoninic acid).

EGFR Immunoprecipitation and Western Blot Analysis. EGFR immunoprecipitations were carried out essentially as described in Ref. 25. Three hundred μg of protein were incubated with an anti-EGFR antibody-agarose conjugate (Santa Cruz Biotechnology, Santa Cruz, CA) for 5 h at 4°C. Immune complexes were washed three times in lysis buffer, resuspended in $1\times$ sample

buffer, and resolved by SDS-PAGE. Western blotting was conducted using anti-phospho-tyrosine (Santa Cruz Biotechnology) or pan-EGFR antibodies (Cell Signaling Technologies) detected by chemiluminescence.

Detection of ROS by EPR and Flow Cytometry. For EPR, subconfluent cells were harvested with trypsin, washed once, and resuspended in cell growth media at 1×10^7 cells/ml. For each EPR scan, 5 μl of 1 M BMPO were added to 94 μl of cell suspension (approximately 1×10^6 cells) and 1 μl of BPQ or DMSO [1% DMSO (v/v), final concentration]. The cell mixture was immediately drawn into gas-permeable Teflon tubing (Zeus Industries, Raritan, NJ), folded several times, and inserted into a quartz EPR tube open at each end. The EPR cavity was maintained at 37°C, and the EPR spectra were obtained with a Bruker Elexsys X-band EPR spectrometer. Typical settings for the spectrometer were as follows: magnetic field, 3200 G; scan range, 60 G; incident microwave power, 15 mW; modulation amplitude, 1 G; and scan time, 160 s. The EPR spectra were collected, stored, and manipulated using the Bruker software Xepr. Intracellular H_2O_2 was measured with H_2DCF-DA (Molecular Probes, Eugene, OR) by flow cytometry. MCF-10A cells were plated into collagen-coated 6-well plates at 1.0×10^5 cells/well and cultured to 70–80% confluence. Cells were loaded with 10 μM DCF-DA in PBS for 15 min and treated as indicated in growth media. After treatment, cells were detached with trypsin, washed once with media, and suspended in media for analysis by flow cytometry (FACScan; Becton Dickinson). Results are expressed as the mean channel fluorescence of 10,000 gated events.

Subcloning and Transfections. The cDNA *SOD1* was obtained from MCF-10A RNA through rt-PCR. *SOD1* cloning was accomplished using PCR primer sequences designed with *Xho*I and *Xba*I restriction enzyme sites for directional cloning into the pCIneo mammalian expression vector (Promega): forward primer, 5'-ATTATT<u>CTCGAG</u>ATGGCGACGAAGGC; and reverse primer, 5'-CCCGGCCT<u>TCTAGA</u>TTTGCCTTCTCCCTTG (restriction sites are *underlined*). Purified plasmids were screened by restriction site analysis and bidirectional sequencing of the cloned insert (University of New Mexico Center for Genetics in Medicine Sequencing Facility, Albuquerque, NM). The cDNA for human CAT was obtained from pCA-CAT (a gift from Dr. Arthur Cederbaum, Mount Sinai School of Medicine, New York, NY) and inserted into the *Sal*I and *Not*I restriction sites of pCIneo. Cells were transiently transfected for 5 h in Ham's F-12 media without serum or other additives using FuGENE 6 transfection reagent (Roche) according to supplied instructions. Cells were allowed to recover for 24 h in complete media before treatment.

Real-Time rt-PCR for HO-1. HO-1 mRNA induction was determined using real-time rt-PCR. MCF-10A cells were plated onto collagen-coated 6-well plates at 1.0×10^5 cells/well. Five days after plating, cells were treated as indicated, and total RNA was collected using the RNeasy Mini RNA isolation kit (Qiagen, Valencia, CA). RNA was eluted into RNase-free water, quantified by UV absorbance, and aliquoted at $-80°C$ until use. rt-PCR was performed on equal amounts of total RNA (25 ng) using the TaqMan Gold One-Step rt-PCR kit (Applied Biosystems, Foster City, CA). TaqMan primers and a 6-carboxyfluorescein-labeled probe were designed using Primer Express software (Applied Biosystems) and a published sequence for HO-1 mRNA (31). Forward primer was 5'-GCCCTTCAGCATCCTCAGTTC, reverse primer was 5'-GGTTTGAGACAGCTGCCACAT, and probe was 5'-6-carboxyfluorescein-TGCAGCAGAGCCTGGAAGACACCC-6-carboxytetra-methylrhodamine. rt-PCR was performed in MicroAmp 96-well Optical Reaction plates (Applied Biosystems) on the Applied Biosystems Prism 7000 Sequence Detection System using the following rt-PCR cycle: 42°C for 30 min and 95°C for 10 min followed by 40 cycles at 95°C for 15 s and 60°C for 1 min. Results are calculated from the mean threshold cycle of triplicate treatments averaged from three replicate PCR reactions and are relative to a standard curve created from various amounts (0–200 ng) of untreated MCF-10A total RNA.

Statistical Analysis. Data were analyzed for statistical differences ($P < 0.05$) between control and treated groups using SigmaStat software (Jandel Scientific, San Rafael, CA). ANOVA followed by Dunnett's *t* tests was performed on sample means.

RESULTS

Effect of BPQs on MCF-10A Cell Number in EGF-Deficient Media. The present studies were undertaken to investigate whether BPQs increase MCF-10A cell number in the absence of EGF, a

7826

response we have previously observed to occur with BaP. In these experiments, cell number was determined with a colorimetric method described in "Materials and Methods." In Fig. 1A, cells were treated with 0.1 μM of either 1,6-BPQ or 3,6-BPQ for 1–6 days in EGF-deficient media. Beginning at 3 days of treatment, BPQs increased cell number when compared with cells treated with only DMSO. A concentration-response analysis conducted after treatment for 4 days found increased cell number from 0.03 to 0.3 μM 1,6-BPQ and from 0.03 to 1.0 μM 3,6-BPQ (Fig. 1B). The concentration response at this treatment time was biphasic; low concentrations of BPQs stimulated cell proliferation, whereas concentrations at 1.0 μM began to be inhibitory.

Characterization of EGFR Activation by BPQs. Because we found BPQ-induced cell proliferation occurred in the absence of EGF (Fig. 1), we evaluated the extent of EGFR activity in treated cells. In Fig. 2, subconfluent cell cultures were treated with either DMSO or 1 μM BPQs, and Western analysis was conducted as described in "Materials and Methods." The *top panel* of Fig. 2A shows that 1,6-BPQ and 3,6-BPQ increased EGFR tyrosine phosphorylation at 12 and 18 h when compared with control cells (*Lanes C*). To determine whether this increased EGFR phosphorylation led to downstream signaling from the receptor, we also assayed for Akt and Erk activity. As demonstrated in Fig. 2A, 1,6-BPQ and 3,6-BPQ increased p-Akt evident at 12 and 18 h. 3,6-BPQ produced significant phosphorylated Erk1,2 beginning at 12 h, whereas 1,6-BPQ only modestly increased Erk1,2 phosphorylation. We did not observe significant
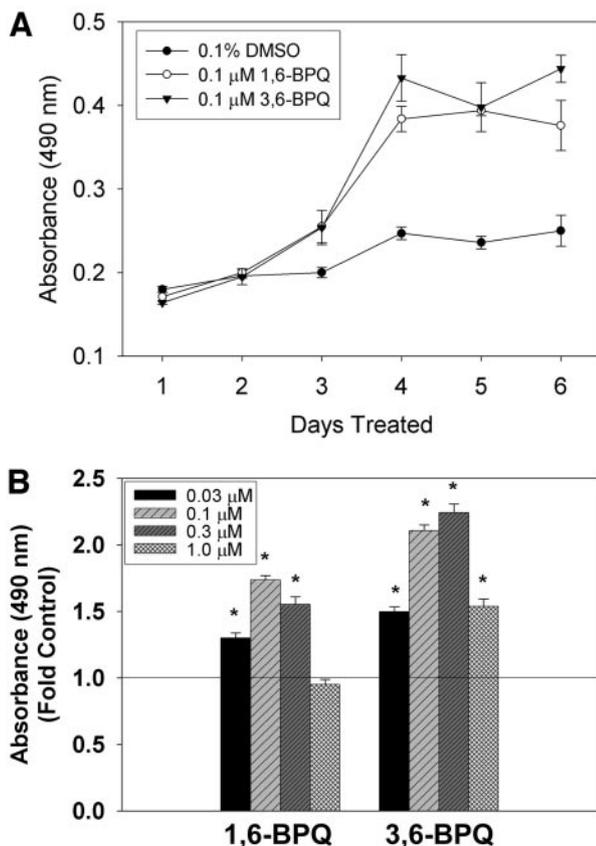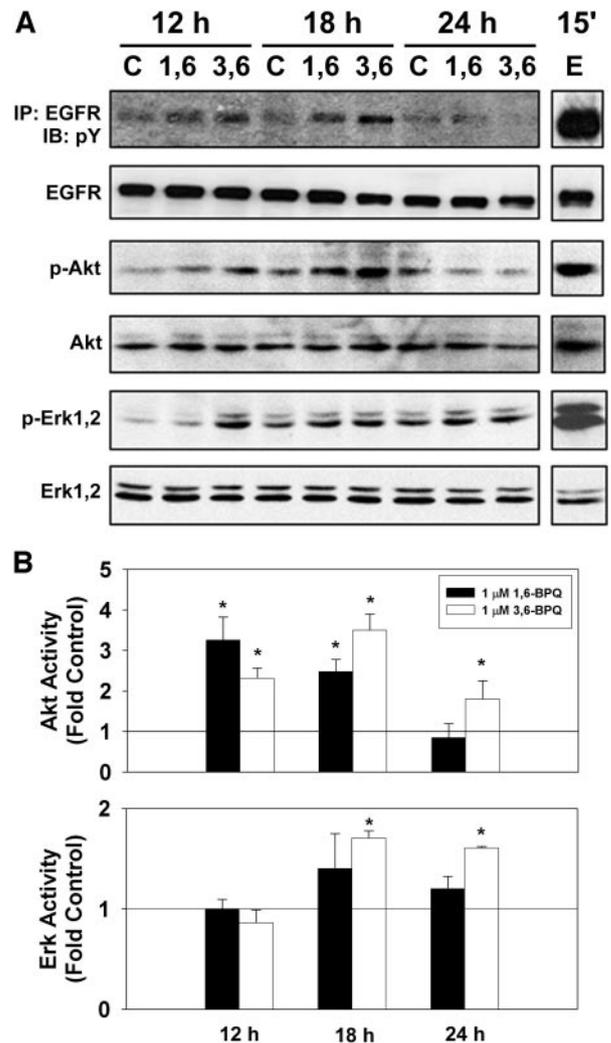

Fig. 2. BPQs increase EGFR pathway activation. *A,* MCF-10A cells were cultured overnight in media without EGF or insulin and treated for 12, 18, or 24 h with 1 μM 1,6-BPQ or 1 μM 3,6-BPQ or for 15 min with 10 ng/ml EGF. Cell lysates were collected, and the EGFR was immunoprecipitated with an EGFR-specific antibody (*IP:EGFR*) and resolved by SDS-PAGE, and EGFR tyrosine phosphorylation was determined by Western blotting with a phospho-Tyr antibody (*IB:pY*). Equal amounts of the remaining cell lysates (10 μg of protein) were separated by SDS-PAGE and probed with phospho-specific or pan-specific antibodies for Akt and Erk1,2. *B,* Akt kinase activity was determined by evaluating the extent of phosphate incorporated into a GSK-3 fusion protein serving as the substrate for immunoprecipitated Akt (*top panel*). Erk activity was determined via an Elk-1 luciferase reporter system as described in the text (*bottom panel*). *C,* DMSO control. *E,* EGF.

Fig. 1. BPQs increase MCF-10A cell proliferation in the absence of EGF. *A* and *B,* MCF-10A cells were cultured and treated in 96-well plates, and cell number was determined by a colorimetric assay as described in "Materials and Methods." *A,* cells were treated from 1 to 6 days in media without EGF in the presence of DMSO (●), 0.1 μM 1,6-BPQ (○), or 0.1 μM 3,6-BPQ (▼). *B,* cell number was determined after treatment for 4 days with 0.03–1.0 μM 1,6-BPQ or 0.03–1.0 μM 3,6-BPQ. *Points* and *bars* are calculated from the mean absorbance at 490 nm ($\pm$SE) in six replicate samples. ∗, significantly different from control ($P < 0.05$).

differences in the total amount of EGFR, Akt, or Erk1,2 protein between treatments (Fig. 2A). However, we found that EGFR phosphorylation induced by BPQs differed from that produced by EGF in terms of the kinetics and signal intensity because treatment of cells with 10 ng/ml EGF produced a rapid (15 min) and more substantial increase in EGFR, Akt, and Erk1,2 phosphorylation (Fig. 2A, *Lane E*).

We verified that Akt was indeed activated in BPQ-treated cells with a nonradioactive kinase assay that used a GSK-3/paramyosin fusion protein as a substrate for immunoprecipitated Akt. The assay confirmed that Akt was activated by BPQs because of the increased proportion of phosphorylated GSK-3 substrate protein detected (Fig. 2B, *top panel*). Similarly, Erk1,2 activity was confirmed by evaluating the transcriptional activity of the Erk substrate, Elk-1, via the transient cotransfection of a chimeric Elk-1/GAL4 expression plasmid and a GAL4-driven luciferase reporter plasmid. The expression plasmid produces an Elk-1/GAL4 fusion protein consisting of the transactivation domain of Elk-1 and the DNA-binding domain of GAL4. The

7827

phosphorylation, and subsequent activation, of the Elk-1/GAL4 fusion protein by endogenous Erk has been shown to increase luciferase reporter activity (32). As shown in the *bottom panel* of Fig. 2*B*, 3,6-BPQ increased reporter activity at 18 and 24 h, confirming that Erk1,2 activity was enhanced by 3,6-BPQ. 1,6-BPQ slightly increased the reporter activity at 18 h; however, this change by 1,6-BPQ was not statistically significant from controls.

Additionally, at 18 h of treatment, 1,6-BPQ and 3,6-BPQ produced concentration-dependent increased EGFR, Akt, and Erk1,2 phosphorylation from 0.03–1.0 μM (Fig. 3*A*). Similar to the results of the Western analysis, BPQs increased Akt and Erk1,2 activities in a concentration-dependent manner as determined by the Akt kinase assay and Elk-1 reporter assay, respectively (Fig. 3*B, top* and *bottom panels*, respectively).

Requirement of EGFR for BPQ-Induced Kinase Activity and Cell Proliferation. We investigated the requirement for the EGFR in BPQ-induced Akt or Erk1,2 activity, as well as cell proliferation, using a highly specific inhibitor of the EGFR kinase, AG1478. In MCF-10A cells, AG1478 produced a marked suppression of EGFR activity induced by 10 ng/ml EGF in a concentration-dependent manner, with complete inhibition of the receptor pathway at the 1 μM concentration of AG1478 (Fig. 4*A*). As expected, the presence of 1 μM AG1478 suppressed EGFR, Akt, and Erk1,2 phosphorylation and kinase activities induced by 1 μM 1,6-BPQ, and 1 μM 3,6-BPQ (Fig. 4*B*). Importantly, AG1478 dose dependently limited the extent of both BPQ- and EGF-induced cell proliferation (Fig. 4*C*).

EPR Detection of O_2^- and Flow Cytometric Detection of H_2O_2 in BPQ-Treated MCF-10A Cells. We wished to determine whether the increased EGFR activity caused by BPQs was because of the production of ROS. Therefore, we chose to use EPR and the spin trap, BMPO (33), to directly measure the presence of free radicals in MCF-10A cells treated with BPQs. Using this method, we found that 1,6-BPQ produced a concentration-dependent EPR signal in MCF-10A that was detected from 2 to 20 μM (Fig. 5, *B–E*). A similar EPR spectrum was produced by 20 μM 3,6-BPQ (Fig. 5*F*) but not by BMPO in the absence of BPQs (Fig. 5*A*) or by the vehicle control, 1% DMSO (Fig. 5*G*). We did not detect EPR signals in the absence of MCF-10A cells (data not shown). The EPR signal was assigned to the BMPO adduct of O_2^- because the spectrum was consistent with the reported spectrum for BMPO/O_2^- (32), and we did not detect a BMPO/methyl radical adduct that would be indicative of the reaction between hydroxyl radicals and DMSO. Furthermore, the addition of 40 units of SOD to the reaction mixture eliminated the EPR signal produced by 10 μM 1,6-BPQ (Fig. 6, *A versus B*), whereas an equal amount of SOD that was first inactivated by heating could not (Fig. 6*C*). This result demonstrated that O_2^- was the primary free radical contributing to the EPR signal produced by BPQs.

The spontaneous and/or enzymatically catalyzed dismutation of O_2^- into H_2O_2 may represent a major outcome of intracellular O_2^-. Therefore, we assayed for H_2O_2 production in BPQ-treated MCF-10A cells. We used an intracellular probe for H_2O_2, H_2DCF-DA, which is oxidized to DCF by H_2O_2. As shown in Fig. 6*D*, we detected significantly increased DCF fluorescence in BPQ- and H_2O_2-treated MCF-10A cells (Fig. 6*D, left panel*), an increase that was attenuated by transiently overexpressing *CAT* but not by transfecting the empty vector (*neo*; Fig. 6*D, right panel*).

Role of ROS Generation in EGFR Activity. To specifically address the role of ROS in the BPQ-dependent activation of the EGFR pathway, we treated MCF-10A cells in the presence of various antioxidants. Treatment of MCF-10A cells in the presence of the antioxidant and glutathione precursor, NAC, reduced the extent of EGFR tyrosine phosphorylation produced by BPQs (Fig. 7*A, top blot*). Although NAC also suppressed Erk1,2 phosphorylation, it appeared to
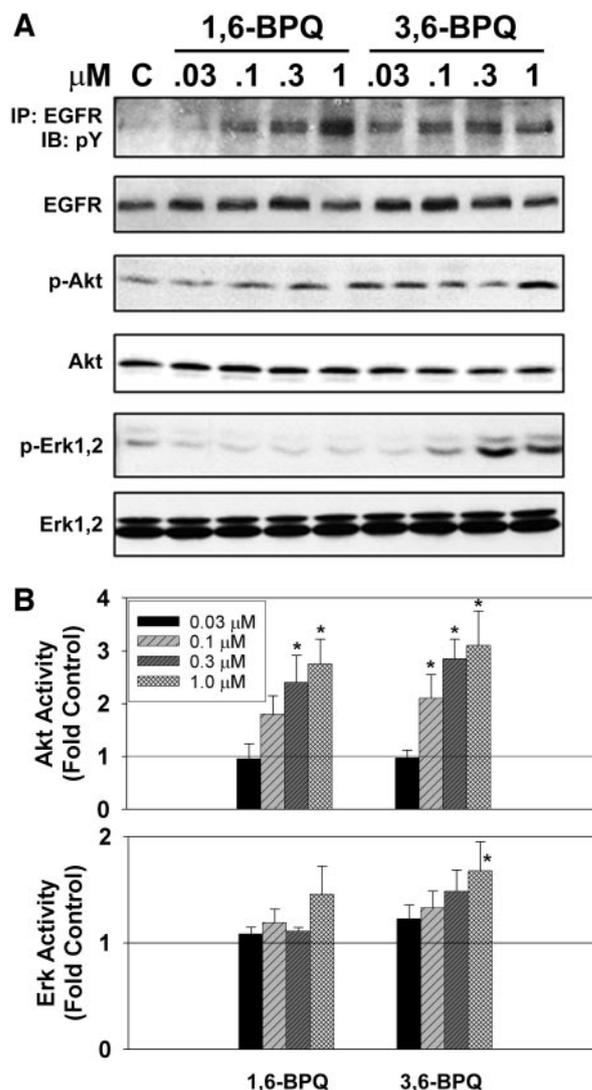

Fig. 3. Concentration-response analysis of EGFR activity. *A,* EGFR, Akt, and Erk1,2 phosphorylation was determined by Western analysis after treating MCF-10A cells 18 h with 0.03–1.0 μM 1,6-BPQ or 0.03–1.0 μM 3,6-BPQ. *B,* Akt and Erk activities were determined in cells treated for 18 h with various concentrations of BPQs as described in the Fig. 2 legend.

have a much greater effect on Akt phosphorylation, essentially eliminating the phospho-Akt signal detected (Fig. 7*A, middle* and *bottom blots*). Consistent with the results of the Western analysis, NAC suppressed Akt and Erk1,2 activities induced by BPQs (Fig. 7*A, bar graphs*). Furthermore, the increased cell number detected after treatment for 4 days with 0.1 μM BPQs was suppressed completely by cotreatment with NAC (Fig. 7*B*).

We used a genetic approach to specifically target intracellular ROS by either transiently overexpressing SOD1 (which catalyzes the dismutation of O_2^- into H_2O_2) or CAT, which converts H_2O_2 to H_2O. EGFR, Akt, and Erk1,2 activity was slight but suppressed repeatedly by transfecting *CAT*, but not *SOD1*, when compared with cells transfected with only the empty vector (Fig. 8*A*). Furthermore, transient transfection with CAT conferred protection from the increased cell growth produced by treatment for 4 days with 0.1 μM BPQs (Fig. 8*C*). We obtained substantial SOD1 and CAT protein overexpression in transiently transfected MCF-10A cells that were maintained through the duration of the cell growth assay (96 h; Fig. 8*B*).

H_2O_2 Transactivates the EGFR in MCF-10A Cells. Given that CAT overexpression in MCF-10A cells was found to decrease EGFR
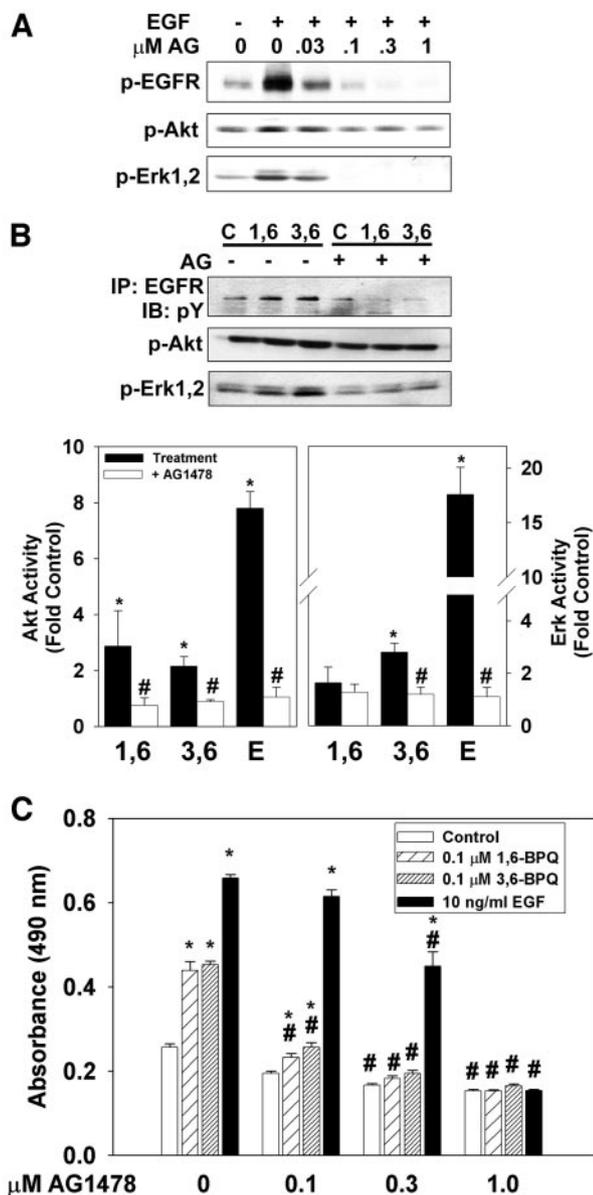
7828

Fig. 4. The EGFR inhibitor AG1478 suppresses EGFR, Akt, and Erk1,2 phosphorylation by BPQs. *A,* MCF-10A cells were cultured overnight in media without EGF or insulin and pretreated for 15 min with 0.03–1.0 μM AG1478, a specific EGFR kinase inhibitor. Cells were treated for 15 min with 10 ng/ml EGF, and EGFR, Akt, and Erk1,2 phosphorylation was determined by Western analysis with phospho-specific antibodies. *B,* EGFR, Akt, and Erk1,2 activity was determined as described in the Fig. 2 legend in MCF-10A cells treated with 1 μM 1,6-BPQ or 1 μM 3,6-BPQ for 18 h in the presence or absence of 1 μM AG1478. *C,* MCF-10A cells were treated for 4 days with 0.1 μM 1,6-BPQ, 0.1 μM 3,6-BPQ, or 10 ng/ml EGF in the presence of increasing amounts of AG1478. Cell number was determined by a colorimetric assay as described in "Materials and Methods." *Bars* represent the mean absorbance at 490 nm ($\pm$SE), $n = 6$. #, significantly different from treatment without AG1478 ($P < 0.05$) *E,* EGF.

signaling in response to BPQ treatment, we assessed whether direct treatment with H_2O_2 activated similar EGFR pathways in MCF-10A. As in previous experiments, cells were cultured overnight in media without EGF or insulin, and the following day, cells were subjected to treatment with 200 μM H_2O_2 for 30 min. As shown in Fig. 9, H_2O_2 significantly increased phosphorylation of the EGFR, Akt, and Erk1,2. Activation of the receptor pathway was inhibited by pretreating with 1 μM AG1478 and 5 mM NAC and suppressed completely with 1000 units/ml CAT.

Measurement of Oxidative Stress in MCF-10A Cells Treated with BPQs. We found that BPQs could increase EGFR pathway activity in a concentration-dependent manner (Fig. 3), yet with respect

to cell number, concentrations of BPQs above 0.3 μM began to be inhibitory (Fig. 1*B*). To explain this inconsistency, we hypothesized that the apparent toxicity of high concentrations of BPQs was because of excessive oxidative stress that may have superseded the prosurvival signal from the EGFR. Therefore, we examined the induction of HO-1 mRNA with real-time rt-PCR because the induction of HO-1 has been reported previously to be a sensitive genetic marker for cellular oxidative stress (34, 35). In the treatment times examined, the greatest induction of HO-1 by 0.3 μM BPQs occurred at 8 h (Fig. 10*A*). A concentration-response analysis conducted at 8 h with 0.1–1.0 μM BPQs found submicromolar concentrations of BPQs to produce <2-fold HO-1 mRNA induction; however, 1 μM BPQs substantially increased HO-1 expression by 10–15-fold (Fig. 10*B*).

DISCUSSION

The major finding of this study was that BPQs activated EGFR signaling pathways and increased cell number in the HMEC line MCF-10A when deprived of EGF. BPQ treatment led to concentration-dependent increased EGFR pathway activation that was prevented by the EGFR kinase inhibitor AG1478, the pharmacological antioxidant NAC, and overexpression of CAT. Using EPR and spin-trapping techniques, we directly identified the production of O_2^- in MCF-10A cells treated with BPQs. Additionally, we observed increased DCF fluorescence in BPQ-treated cells that indicated O_2^- formation resulted in H_2O_2 production. Transient overexpression of CAT, but not SOD1, reduced EGFR pathway activation and protected cells from BPQ-induced increased cell number. Furthermore, direct treatment of MCF-10A cells with H_2O_2 produced a similar pattern of
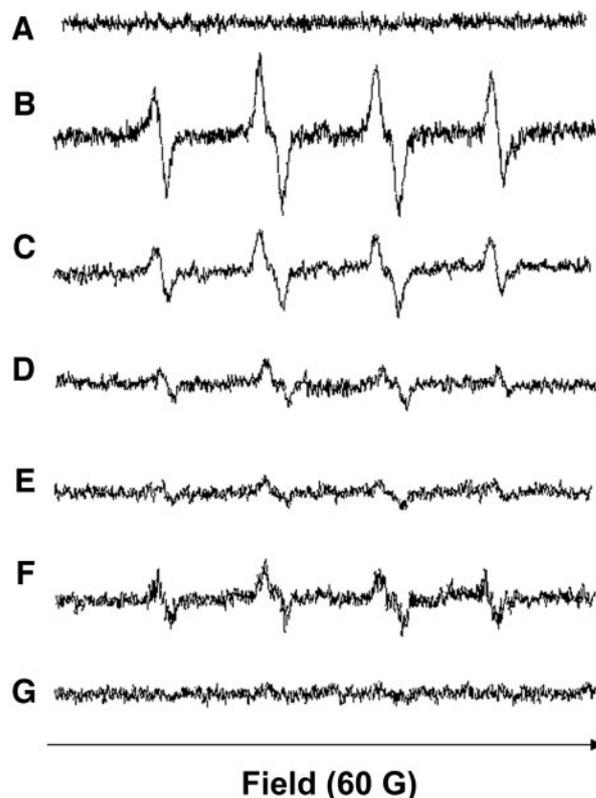

Fig. 5. EPR detection of superoxide anion produced by BPQs in MCF-10A cells. *A–G,* MCF-10A cells were cultured in 100-mm dishes and suspended with trypsin immediately before the assay. EPR was conducted using 1×10^6 cells as described in "Materials and Methods" under the following treatment conditions: *A,* 50 mM BMPO; *B,* BMPO + 20 μM 1,6-BPQ; *C,* BMPO + 10 μM 1,6-BPQ; *D,* BMPO + 5 μM 1,6-BPQ; *E,* BMPO + 2 μM 1,6-BPQ; *F,* BMPO + 20 μM 3,6-BPQ; *G,* BMPO + 1% DMSO.
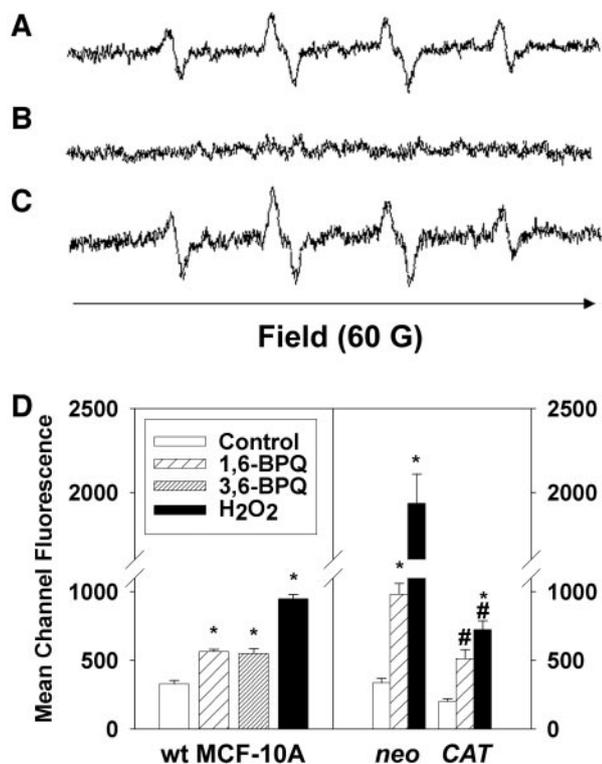
7829

Fig. 6. EPR characterization of superoxide anion and flow cytometric detection of H_2O_2 in BPQ-treated MCF-10A cells. *A–C,* MCF-10A cells were analyzed by EPR as described in the Fig. 5 legend. Treatments were as follows: *A,* 50 mM BMPO + 10 μM 1,6-BPQ; *B,* BMPO + 10 μM 1,6-BPQ and 40 units SOD; *C,* BMPO + 10 μM 1,6-BPQ and 40 units of heat-denatured SOD. *D,* H_2O_2 was measured in MCF-10A cells using the fluorescent probe DCF-DA and flow cytometry as described in "Materials and Methods." *Left panel,* cells were treated for 2 h with 1 μM BPQs or 200 μM H_2O_2. *Right panel,* in a separate experiment, cells were transiently transfected with *CAT* or the empty vector (*neo*) and allowed to recover for 24 h before treatment. Cells were treated for 2 h with 1 μM 1,6-BPQ or 200 μM H_2O_2. *Bars* represent the mean channel fluorescence in triplicate samples. #, significantly different from pCIneo ($P < 0.05$). *Wt,* wild-type.

EGFR pathway activation that was also inhibited by AG1478, NAC, and CAT. Taken together, our data indicated that EGFR activation in MCF-10A cells was mediated by H_2O_2 produced from the O_2^- generated during BPQ redox cycling.

There is substantial evidence that H_2O_2 can lead to phosphorylation and activation of the EGFR pathway. The mechanism by which this occurs is not well defined and often differs from ligand binding with respect to the profile of tyrosine residues that are phosphorylated (36, 37). For example, Ravid *et al.* (38) demonstrated recently that a lack of phosphorylation at EGFR Tyr[1045] by H_2O_2 may prevent proper receptor ubiquitination and degradation, ultimately leading to stably activated receptors at the cell surface. This finding may be particularly noteworthy with respect to our observations because it is plausible that the gradual accumulation of activated cell surface receptors results in a transient increase in EGFR activity. However, BPQ-induced EGFR tyrosine phosphorylation also appears to be at least partially due to increased phosphorylation at the autophosphorylation sites, since AG1478 reduced the amount of phospho-Tyr detected (Fig. 4*B*). The inactivation of phosphatases by H_2O_2 through oxidation of critical sulfhydryl residues in their active sites may represent an additional mechanism for EGFR pathway activation. For example, phosphatase and tensin homologue, which acts as a negative regulator of PI3-K by removing the 3'-phosphate of phosphoinositides, was shown to be reversibly inactivated by H_2O_2 through a disulfide oxidation (39). Furthermore, the EGFR phosphatase PTP1B is a likely target of oxidation by endogenous ROS produced during normal cell signaling (23, 40). These pathways may be particularly sensitive to

low concentrations of exogenous H_2O_2 that may mimic normal cell signaling. The observation that NAC, a strong cellular reductant, was found to block EGFR, Akt, and Erk activity induced by BPQs (Fig. 7) suggests that this is a plausible mechanism in our model.

In our studies, BPQs required substantially longer treatment times than H_2O_2 to enhance EGFR activation. Specifically, we found maximal BPQ-induced EGFR tyrosine phosphorylation to occur between 12 and 18 h, whereas H_2O_2 increased EGFR phosphorylation at 30 min (Fig. 2*A versus* Fig. 9). The differences in the concentrations of H_2O_2 produced by each treatment and the mechanism by which it is delivered likely play a large role in this discrepancy. It is noteworthy that CAT overexpression reduced DCF fluorescence induced by H_2O_2 and 1,6-BPQ (Fig. 6*D, right panel*), verifying the specificity of DCF for H_2O_2 in our cell model. These results also indicate that the overexpression of CAT lowered the steady-state levels of H_2O_2 produced by BPQs, but it did not completely inhibit BPQ redox cycling. As such, CAT overexpression reduced, but did not completely reverse, EGFR activation (Fig. 8*A*) and the increased cell number induced by BPQs (Fig. 8*C*). Our results demonstrating that SOD1 overexpression could not attenuate these responses would be expected if H_2O_2 were ultimately responsible for the activation of the EGFR pathway.

We noted that 3,6-BPQ resulted in greater Akt and Erk activity compared with similar concentrations of 1,6-BPQ. Although both BPQs are derived from BaP, they are unique compounds that may have different signaling capabilities based on their redox potentials
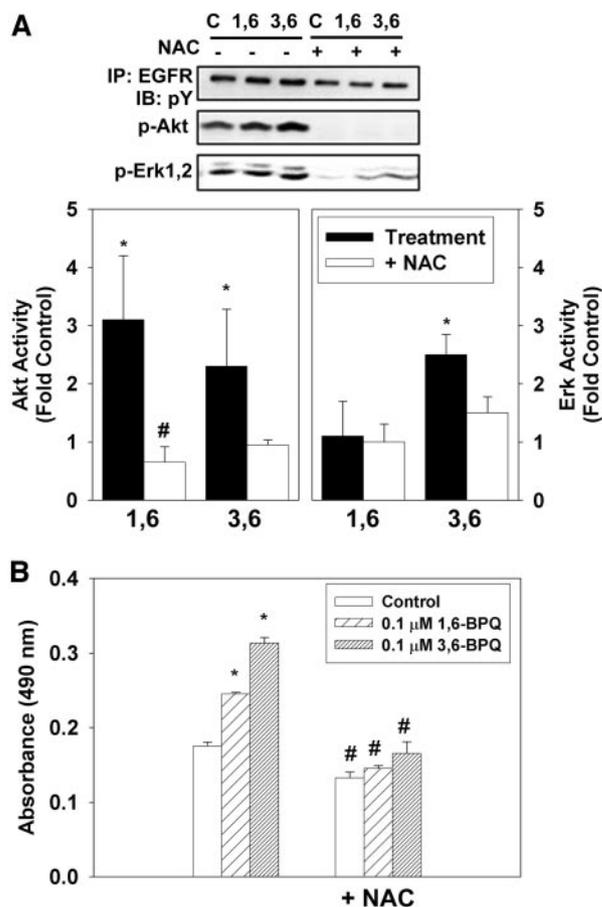

Fig. 7. BPQ-induced EGFR activity and cell proliferation is prevented by NAC. *A,* EGFR, Akt, and Erk1,2 activity was determined as described in previous experiments in cells treated for 18 h with 1 μM BPQs or with BPQs and 5 mM NAC. *B,* MCF-10A cell number was determined after treatment of 4 days with 0.1 μM 1,6-BPQ or 0.1 3,6-BPQ in the presence or absence of 5 mM NAC in EGF-deficient media. #, significantly different from treatment without NAC ($P < 0.05$).

7830

differences in signaling we observed between two similar concentrations of BPQs.

Although BPQs produced concentration-dependent EGFR pathway activation from 0.03 to 1.0 μM (Fig. 3), cell number decreased as BPQ concentrations approached 1 μM (Fig. 1*B*). To explain this, we believe that the higher concentrations of BPQs resulted in increased oxidative stress that could not be overcome by activation of the EGFR pathway. As one such indicator of oxidative stress, we measured the induction of HO-1 and found that BPQ concentrations above 0.3 μM led to significant HO-1 mRNA induction, whereas low concentrations of BPQs did not (Fig. 10). Given that EGFR blockade by AG1478 prevented the increase in cell number (Fig. 4*C*), we believe that the activation of the EGFR pathway represented a prosurvival response to BPQs. This observation is consistent with that of other laboratories that have shown EGFR-dependent Akt activity protected cells from
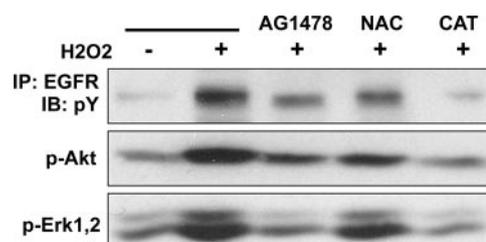
Fig. 9. H_2O_2 treatment increases EGFR, Akt, and Erk1,2 phosphorylation in MCF-10A cells. Subconfluent MCF-10A cells were cultured overnight in media without EGF or insulin, and the following day, the cells were subjected to 30-min treatments with 200 μM H_2O_2, 200 μM H_2O_2 and 1 μM AG1478, 200 μM H_2O_2 and 5 mM NAC, or 200 μM H_2O_2 and 500 units/ml CAT. EGFR, Akt, and Erk1,2 phosphorylation was determined by Western analysis using phospho-specific antibodies.
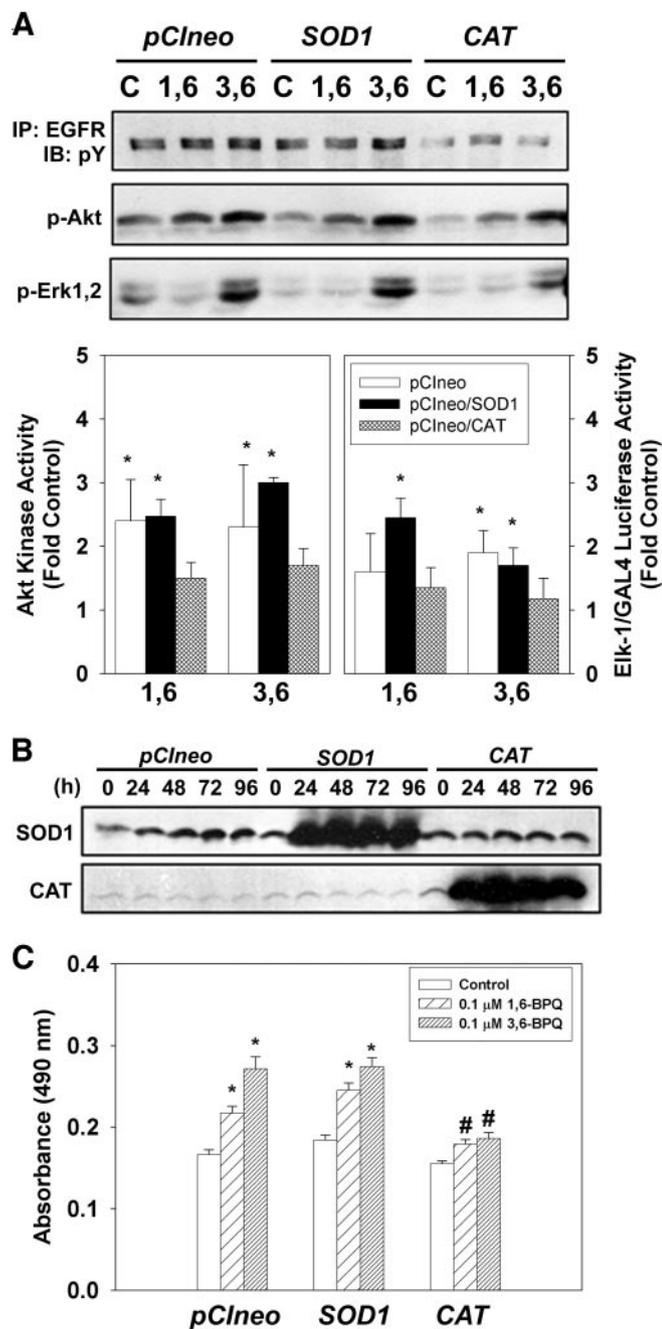
Fig. 8. CAT overexpression prevents BPQ-induced EGFR activity and cell proliferation. *A*, MCF-10A cells were transiently transfected with *CAT*, *SOD1*, or the empty vector (*pCIneo*) and allowed to recover for 24 h before treatment. As described in the Fig. 7 legend, the extent of EGFR, Akt, and Erk1,2 activity was determined in cells treated for 18 h with 1 μM BPQs. *B*, transfected cells were harvested into lysis buffer immediately (0), 24, 48, 72, or 96 h after transfection, and SOD1 and CAT protein expression was determined by Western analysis. *C*, cells were transiently transfected with *pCIneo/CAT*, *pCIneo/SOD1*, or the empty vector and allowed to recover for 24 h before treatment. Cell number was determined after treatment for 4 days with 0.1 μM BPQs in EGF-deficient media. #, significantly different from pCIneo ($P < 0.05$).

and/or abilities to interact with other signaling pathways. Interestingly, we have evidence that 3,6-BPQ can enhance AhR activity in MCF-10A cells.[2] This may prove significant because we have demonstrated previously that the AhR ligand 2,3,7,8-tetrachlorodibenzo-*p*-dioxin can up-regulate transforming growth factor α in an AhR-dependent manner, leading to autocrine signaling through the EGFR in MCF-10A (30, 41). This mechanism may represent an additional pathway for EGFR activation by 3,6-BPQ that may account for the

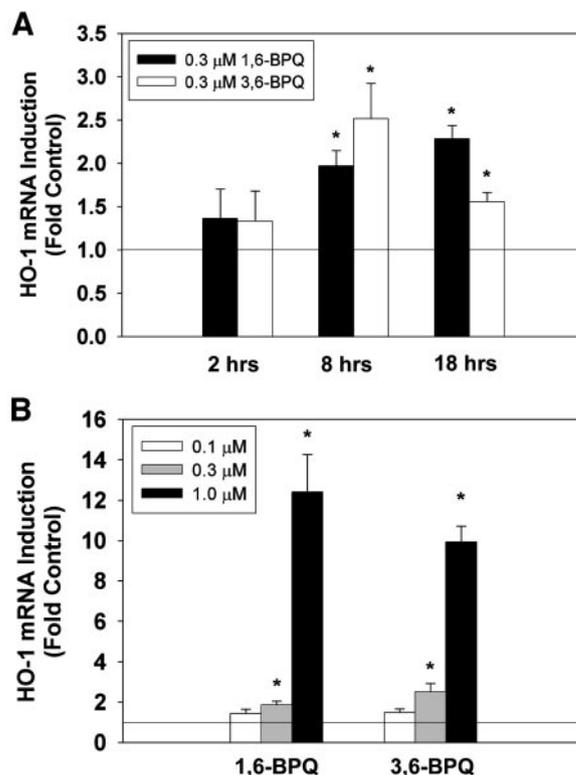Fig. 10. BPQs increase HO-1 expression. *A* and *B*, total RNA (25 ng) was collected from treated cells and subjected to real-time rt-PCR using HO-1-specific primers and a fluorescence-labeled probe. Cells were treated as follows: *A*, 0.3 μM 1,6-BPQ or 0.3 μM 3,6-BPQ for 2, 8, and 18 h; and *B*, 0.03, 0.3, and 3 μM 1,6-BPQ or 0.03, 0.3, and 3 μM 3,6-BPQ for 8 h. Data represent the mean fold increase in HO-1 mRNA calculated from triplicate samples and three replicate PCR reactions.

7831

H_2O_2-induced apoptosis (25). It is also important to note that concentrations of BPQs above 0.3 μM only exhibited signs of toxicity after 4 days of sustained treatment. At the time of maximal EGFR phosphorylation (18 h), we did not detect decreased cell viability by 1 μM BPQs (data not shown).

We have determined previously that EGF withdrawal from MCF-10A cultures resulted in increased apoptotic cells beginning at 3 days (28). This time frame corresponded to the period in which we first observed increased cell number in BPQ-treated cells (Fig. 1B). Although we did not specifically address the mechanism for increased cell number in these studies, we believe it is at least partially because of Akt activity and the subsequent inhibition of EGF withdrawal-induced apoptosis. Akt has been shown to exert an antiapoptotic role in cell signaling through multiple mechanisms, including the phosphorylation and inactivation of apoptotic mediators such as Bad, caspase-9, and the Forkhead family of transcription factors (42–44). Furthermore, we have observed that BPQs prevent EGF withdrawal-induced poly(ADP-ribose) polymerase cleavage that can be restored by pharmacological PI3-K inhibitors.[2] This suggests PI3-K/Akt may be inhibiting these apoptotic mediators in BPQ-treated cells because poly(ADP-ribose) polymerase is a known downstream target of active caspases. However, we cannot disregard the possibility that the Erk1,2 pathway also provides an additional mitogenic stimuli. Additional studies on this topic will be necessary to determine the exact pathways leading to increased cell number.

We have shown previously that BaP can act as a weak mitogen in primary HMECs and in the MCF-10A cell line in the absence of exogenously added growth factors (26, 27). However, we hypothesized that the effects observed previously with BaP were because of the production of oxidative metabolites, with greater biological activity. It is interesting to note that the concentrations of BPQs that increased MCF-10A cell proliferation in these studies (0.03–0.1 μM) were approximately 10-fold lower than those required for BaP to produce similar results. This is significant because we hypothesize that BaP is metabolized to BPQs in HMECs. Therefore, BPQs may play a significant role in the ability of BaP to activate growth factor receptor pathways and increase cell number in HMECs cultured in the absence of growth factors. Although we specifically addressed the activation of the EGFR pathway in MCF-10A, it is likely that BPQ-induced responses are not limited to this particular growth factor receptor. In fact, we have shown that BaP can also increase tyrosine phosphorylation of the insulin-like growth factor I receptor β in MCF-10A (27), a response that may also be ROS dependent.

In summary, the experimental evidence presented here demonstrates that BPQs enhanced EGFR pathway activation in mammary epithelial cells by redox cycling to produce O_2^- and ultimately H_2O_2. Specifically, our data indicate that H_2O_2 plays a role in EGFR activation by BPQs. These results may provide novel insights into the mechanisms by which metabolites of BaP may contribute to tumor promotion and, ultimately, mammary carcinogenesis.

ACKNOWLEDGMENTS

REFERENCES

1. Alberg, A. J., Singh, S., May, J. W., and Helzlsouer, K. J. Epidemiology, prevention, and early detection of breast cancer. Curr. Opin. Oncol., *12:* 515–520, 2000.
2. el Bayoumy, K. Environmental carcinogens that may be involved in human breast cancer etiology. Chem. Res. Toxicol., *5:* 585–590, 1992.
3. Dipple, A. Formation, metabolism, and mechanism of action of polycyclic aromatic hydrocarbons. Cancer Res., *43* (Suppl.)*:* 2422s–2425s, 1983.
4. Gould, M. N., Grau, D. R., Seidman, L. A., and Moore, C. J. Interspecies comparison of human and rat mammary epithelial cell-mediated mutagenesis by polycyclic aromatic hydrocarbons. Cancer Res., *46:* 4942–4945, 1986.
5. Ethier, S. P., and Ullrich, R. L. Induction of mammary tumors in virgin female BALB/c mice by single low doses of 7,12-dimethylbenz[*a*]anthracene. J. Natl. Cancer Inst. (Bethesda), *69:* 1199–1203, 1982.
6. Russo, J., Tahin, Q., Lareef, M. H., Hu, Y. F., and Russo, I. H. Neoplastic transformation of human breast epithelial cells by estrogens and chemical carcinogens. Environ. Mol. Mutagen., *39:* 254–263, 2002.
7. Jeffrey, A. M., Jennette, K. W., Blobstein, S. H., Weinstein, I. B., Beland, F. A., Harvey, R. G., Kasal, H., Miura, I., and Nakanishi, K. Benzo[*a*]pyrene-nucleic acid derivative found *in vivo*: structure of a benzo[*a*]pyrenetetrahydrodiol epoxide-guanosine adduct. J. Am. Chem. Soc., *98:* 5714–5715, 1976.
8. Denissenko, M. F., Pao, A., Tang, M., and Pfeifer, G. P. Preferential formation of benzo[*a*]pyrene adducts at lung cancer mutational hotspots in P53. Science (Wash. DC), *274:* 430–432, 1996.
9. Marshall, C. J., Vousden, K. H., and Phillips, D. H. Activation of c-Ha-*ras*-1 proto-oncogene by *in vitro* modification with a chemical carcinogen, benzo(*a*)pyrene diol-epoxide. Nature (Lond.), *310:* 586–589, 1984.
10. Rundle, A., Tang, D., Hibshoosh, H., Estabrook, A., Schnabel, F., Cao, W., Grumet, S., and Perera, F. P. The relationship between genetic damage from polycyclic aromatic hydrocarbons in breast tissue and breast cancer. Carcinogenesis (Lond.), *21:* 1281–1289, 2000.
11. Conney, A. H. Induction of microsomal enzymes by foreign chemicals and carcinogenesis by polycyclic aromatic hydrocarbons: G. H. A. Clowes Memorial Lecture. Cancer Res., *42:* 4875–4917, 1982.
12. Reed, M. D., Monske, M. L., Lauer, F. T., Meserole, S. P., Born, J. L., and Burchiel, S. W. Benzo[*a*]pyrene diones are produced by photochemical and enzymatic oxidation and induce concentration-dependent decreases in the proliferative state of human pulmonary epithelial cells. J. Toxicol. Environ. Health Part A, *66:* 1189–1205, 2003.
13. Lorentzen, R. J., and Ts'o, P. O. Benzo[*a*]renedione/benzo[*a*]pyrenediol oxidation-reduction couples and the generation of reactive reduced molecular oxygen. Biochemistry, *16:* 1467–1473, 1977.
14. Flowers, L., Ohnishi, S. T., and Penning, T. M. DNA strand scission by polycyclic aromatic hydrocarbon *o*-quinones: role of reactive oxygen species, Cu(II)/Cu(I) redox cycling, and *o*-semiquinone anion radicals. Biochemistry, *36:* 8640–8648, 1997.
15. Burchiel, S. W., and Luster, M. I. Signaling by environmental polycyclic aromatic hydrocarbons in human lymphocytes. Clin. Immunol., *98:* 2–10, 2001.
16. Bolton, J. L., Trush, M. A., Penning, T. M., Dryhurst, G., and Monks, T. J. Role of quinones in toxicology. Chem. Res. Toxicol., *13:* 135–160, 2000.
17. Ramos, K. S. Redox regulation of c-Ha-*ras* and osteopontin signaling in vascular smooth muscle cells: implications in chemical atherogenesis. Annu. Rev. Pharmacol. Toxicol., *39:* 243–265, 1999.
18. Aust, S. D., Chignell, C. F., Bray, T. M., Kalyanaraman, B., and Mason, R. P. Free radicals in toxicology. Toxicol. Appl. Pharmacol., *120:* 168–178, 1993.
19. Finkel, T. Oxygen radicals and signaling. Curr. Opin. Cell Biol., *10:* 248–253, 1998.
20. Rhee, S. G. Redox signaling: hydrogen peroxide as intracellular messenger. Exp. Mol. Med., *31:* 53–59, 1999.
21. Hayes, G. R., and Lockwood, D. H. Role of insulin receptor phosphorylation in the insulinomimetic effects of hydrogen peroxide. Proc. Natl. Acad. Sci. USA, *84:* 8115–8119, 1987.
22. Goldkorn, T., Balaban, N., Matsukuma, K., Chea, V., Gould, R., Last, J., Chan, C., and Chavez, C. EGF-receptor phosphorylation and signaling are targeted by H_2O_2 redox stress. Am. J. Respir. Cell Mol. Biol., *19:* 786–798, 1998.
23. Bae, Y. S., Kang, S. W., Seo, M. S., Baines, I. C., Tekle, E., Chock, P. B., and Rhee, S. G. Epidermal growth factor (EGF)-induced generation of hydrogen peroxide. Role in EGF receptor-mediated tyrosine phosphorylation. J. Biol. Chem., *272:* 217–221, 1997.
24. Guyton, K. Z., Liu, Y., Gorospe, M., Xu, Q., and Holbrook, N. J. Activation of mitogen-activated protein kinase by H_2O_2. Role in cell survival following oxidant injury. J. Biol. Chem., *271:* 4138–4142, 1996.
25. Wang, X., McCullough, K. D., Franke, T. F., and Holbrook, N. J. Epidermal growth factor receptor-dependent Akt activation by oxidative stress enhances cell survival. J. Biol. Chem., *275:* 14624–14631, 2000.
26. Tannheimer, S. L., Barton, S. L., Ethier, S. P., and Burchiel, S. W. Carcinogenic polycyclic aromatic hydrocarbons increase intracellular Ca^{2+} and cell proliferation in primary human mammary epithelial cells. Carcinogenesis (Lond.), *18:* 1177–1182, 1997.
27. Tannheimer, S. L., Ethier, S. P., Caldwell, K. K., and Burchiel, S. W. Benzo-[*a*]pyrene- and TCDD-induced alterations in tyrosine phosphorylation and insulin-like growth factor signaling pathways in the MCF-10A human mammary epithelial cell line. Carcinogenesis (Lond.), *19:* 1291–1297, 1998.
28. Davis, J. W., Melendez, K., Salas, V. M., Lauer, F. T., and Burchiel, S. W. 2,3,7,8-Tetrachlorodibenzo-*p*-dioxin (TCDD) inhibits growth factor withdrawal-induced apoptosis in the human mammary epithelial cell line, MCF-10A. Carcinogenesis (Lond.), *21:* 881–886, 2000.
29. Cory, A. H., Owen, T. C., Barltrop, J. A., and Cory, J. G. Use of an aqueous soluble tetrazolium/formazan assay for cell growth assays in culture. Cancer Commun., *3:* 207–212, 1991.
30. Davis, J. W., Lauer, F. T., Burdick, A. D., Hudson, L. G., and Burchiel, S. W. Prevention of apoptosis by 2,3,7,8-tetrachlorodibenzo-*p*-dioxin (TCDD) in the MCF-

10A cell line: correlation with increased transforming growth factor α production. Cancer Res., *61:* 3314–3320, 2001.

31. Yoshida, T., Biro, P., Cohen, T., Muller, R. M., and Shibahara, S. Human heme oxygenase cDNA and induction of its mRNA by hemin. Eur. J. Biochem., *171:* 457–461, 1988.

32. Marais, R., Wynne, J., and Treisman, R. The SRF accessory protein Elk-1 contains a growth factor-regulated transcriptional activation domain. Cell, *73:* 381–393, 1993.

33. Zhao, H., Joseph, J., Zhang, H., Karoui, H., and Kalyanaraman, B. Synthesis and biochemical applications of a solid cyclic nitrone spin trap: a relatively superior trap for detecting superoxide anions and glutathiyl radicals. Free Radic. Biol. Med., *31:* 599–606, 2001.

34. Li, N., Venkatesan, M. I., Miguel, A., Kaplan, R., Gujuluva, C., Alam, J., and Nel, A. Induction of heme oxygenase-1 expression in macrophages by diesel exhaust particle chemicals and quinones via the antioxidant-responsive element. J. Immunol., *165:* 3393–3401, 2000.

35. Tyrrell, R. M., and Basu-Modak, S. Transient enhancement of heme oxygenase 1 mRNA accumulation: a marker of oxidative stress to eukaryotic cells. Methods Enzymol., *234:* 224–235, 1994.

36. Gamou, S., and Shimizu, N. Hydrogen peroxide preferentially enhances the tyrosine phosphorylation of epidermal growth factor receptor. FEBS Lett., *357:* 161–164, 1995.

37. Chen, K., Vita, J. A., Berk, B. C., and Keaney, J. F., Jr. c-Jun *N*-terminal kinase activation by hydrogen peroxide in endothelial cells involves SRC-dependent epidermal growth factor receptor transactivation. J. Biol. Chem., *276:* 16045–16050, 2001.

38. Ravid, T., Sweeney, C., Gee, P., Carraway, K. L., III, and Goldkorn, T. Epidermal growth factor receptor activation under oxidative stress fails to promote c-Cbl mediated down-regulation. J. Biol. Chem., *277:* 31214–31219, 2002.

39. Lee, S. R., Yang, K. S., Kwon, J., Lee, C., Jeong, W., and Rhee, S. G. Reversible inactivation of the tumor suppressor PTEN by H_2O_2. J. Biol. Chem., *277:* 20336–20342, 2002.

40. Lee, S. R., Kwon, K. S., Kim, S. R., and Rhee, S. G. Reversible inactivation of protein-tyrosine phosphatase 1B in A431 cells stimulated with epidermal growth factor. J. Biol. Chem., *273:* 15366–15372, 1998.

41. Davis, J. W., Burdick, A. D., Lauer, F. T., and Burchiel, S. W. The aryl hydrocarbon receptor antagonist, 3′methoxy-4′nitroflavone, attenuates 2,3,7,8-tetrachlorodibenzo-*p*-dioxin-dependent regulation of growth factor signaling and apoptosis in the MCF-10A cell line. Toxicol. Appl. Pharmacol., *188:* 42–49, 2003.

42. Datta, S. R., Dudek, H., Tao, X., Masters, S., Fu, H., Gotoh, Y., and Greenberg, M. E. Akt phosphorylation of BAD couples survival signals to the cell-intrinsic death machinery. Cell, *91:* 231–241, 1997.

43. Cardone, M. H., Roy, N., Stennicke, H. R., Salvesen, G. S., Franke, T. F., Stanbridge, E., Frisch, S., and Reed, J. C. Regulation of cell death protease caspase-9 by phosphorylation. Science (Wash. DC), *282:* 1318–1321, 1998.

44. Kops, G. J., Medema, R. H., Glassford, J., Essers, M. A., Dijkers, P. F., Coffer, P. J., Lam, E. W., and Burgering, B. M. Control of cell cycle exit and entry by protein kinase B-regulated forkhead transcription factors. Mol. Cell. Biol., *22:* 2025–2036, 2002.

Benzo(*a*)pyrene Quinones Increase Cell Proliferation, Generate Reactive Oxygen Species, and Transactivate the Epidermal Growth Factor Receptor in Breast Epithelial Cells

Andrew D. Burdick, John W. Davis II, Ke Jian Liu, et al.

Updated version	Access the most recent version of this article at: http://cancerres.aacrjournals.org/content/63/22/7825

Cited articles	This article cites 43 articles, 15 of which you can access for free at: http://cancerres.aacrjournals.org/content/63/22/7825.full#ref-list-1
Citing articles	This article has been cited by 8 HighWire-hosted articles. Access the articles at: http://cancerres.aacrjournals.org/content/63/22/7825.full#related-urls

E-mail alerts	Sign up to receive free email-alerts related to this article or journal.
Reprints and Subscriptions	To order reprints of this article or to subscribe to the journal, contact the AACR Publications Department at pubs@aacr.org.
Permissions	To request permission to re-use all or part of this article, use this link http://cancerres.aacrjournals.org/content/63/22/7825. Click on "Request Permissions" which will take you to the Copyright Clearance Center's (CCC) Rightslink site.